Catalysis Letters Vol. 100, Nos. 3–4, April 2005 (© 2005)
DOI: 10.1007/s10562-004-3448-3

'Ethane oxychlorination' over γ-Al_2O_3 supported $CuCl_2$–KCl–$LaCl_3$

L. Xueju, L. Jie, Z. Guangdong, Z. Kaiji, L. Wenxing, and C. Tiexin*

College of Chemistry, Jilin University, Changchun, 130021 P.R. China

Received 28 June 2004; accepted 12 December 2004

A study on γ-Al_2O_3 supported $CuCl_2$/KCl/$LaCl_3$ for ethane oxychlorination was carried out by means of XRD, XPS,TGA/DTA, BET TEM and ICP. The experimental results indicate that the catalytic properties of the 5 wt,%Cu–6 wt.%K–5 wt.%La/γ-$A1_2O_3$ are optimal. This catalyst was studied in more detail and it was found that deactivation of the catalyst was due to carbon deposition and loss of active species of Cu^{+2}.

KEY WORDS: ethane; oxychlorination; ethylene chloride.

1. Introduction

Copper chloride has been a typical catalyst for oxychlorination reaction of hydrocarbon. Since the discovery that copper chloride catalyzes the conversion of hydrogen chloride to chlorine in the Deacon process, much work has been done on the oxychlorination reaction of methane and ethylene [1–4]. However, ethane oxychlorination is promising for developing a rational technology of ethylene chloride production, because ethane as a raw material is cheaper than ethylene [5,6]. Despite the different temperature ranges in which these reactions are carried out: 473–573 K for ethylene oxychlorination, 623–723 K for the methane oxychlorination, and 723–773 K for ethane oxychlorination, the same promoters (potassium chloride and rare-earth chloride) are usually considered to show the same function for these reactions. One of the roles played by the rare-earth elements is to prevent agglomeration. In an electron microscopic study of copper chloride–potassium chloride mixtures supported on low area Al_2O_3 and TiO_2, the mobility of clusters leading to agglomeration at temperatures above 673 K was observed [7], upon addition of rare-earth elements the catalysts showed a decreasing tendency to agglomerate.

The purpose of this work is to investigate effect of lanthanum on the catalytic activity and selectivity for ethane oxychlorination and to illuminate the reason for the deactivation of the above-mentioned optimal catalyst after reaction for 100 h.

2.1 Experimental

2.1. Catalysts preparation and characterization

Commercial γ-Al_2O_3 (specific surface area: 200 m^2/g, pore volume: 0.37 cm^3/g) was chosen as the support. An aqueous solution containing $CuCl_2 \cdot 2H_2O$, KCl and $LaCl_3$ was used to impregnate the support by an incipient wetness method. The. samples were dried at 393 K in air for 2 h, followed by calcination in a muffle furnace at 823 K for 4 h. The prepared catalysts were stored in a desiccator.

Same content of 5 wt.% copper and 6 wt.% potassium and variable contents 0,1,3,5,7 and 9 wt.% of lanthanum are adopted for preparation of the series of catalysts [8], which are denoted as CuKXLa, Where X represents weight percentage of La, for example, CuK3La stands for a catalyst containing 5 wt.% Cu, 6 wt.% K and 3 wt.% La.

XRD patterns of this series of catalysts were collected at room temperature by a Shimadzu XRD-6000 X-ray powder diffractometer using Ni-filtered Cu K α radiation at 40 kV and 30 mA in a 2θ range of 10° –80° at a scanning rate of 4°/min.

The oxidation states of copper before and after the reaction were characterized by X-ray photoelectron spectroscopy(XPS; VG ESCA Mark II) using AlKα radiation.

TGA/DTA technique was utilized to investigate the weight loss and the thermal transformations of the catalysts. The amount of carbon deposited on the catalysts was determined using a thermo-gravimetric analyzer (TGA; Perkin-Elmer TGA7) and a differential thermal analyzer (DTA; Perkin-Elmer DTA 1700).

The measurements of the specific surface area of the catalysts were conducted by BET method on MICROMERITICS ASAP-2012 using nitrogen as adsorbate at liquid nitrogen temperature.

Transmission electron microscopic (TEM) images of the catalysts were obtained using a HITACHI-8100IV electron microscope operated at 200 KV. The catalysts were ground in an agate mortar and suspended in cyclohexane [9]. After ultrasonic dispersion one drop of the sample suspension was mounted on a copper grid.

* To whom correspondence should be addressed.
E-mail: ctx@mail.jlu.edu.cn

ICP determinations of the catalysts were made using a PLASMA ICP-1000 spectrometer.

2.2 Catalytic properties test

The catalytic properties of the catalysts for the topic reaction were tested in a tubular fixed-bed continuous flow quartz reactor. A thermocouple was placed in the center of the catalyst bed to monitor the reaction temperature. The reactant mixture consisted of C_2H_6, HCl and air at a volume ratio of C_2H_6:HCl: air = 1:3:5 and a total flowrate of 36 ml/min was used. 1 g catalyst was used in each run. The catalyst was pre-treated in an HCl–air mixture at 773 K for 30 min [10]. The reaction were run at 773 K.

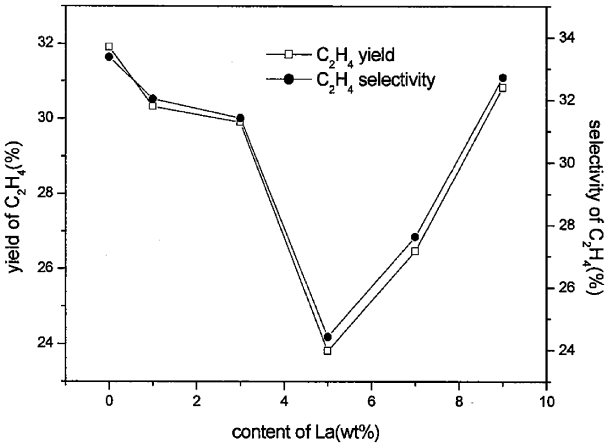

Figure 2. Influence of content of La on the yield and selectivity of C_2H_4.

3. Results and discussion

3.1. Catalytic properties for ethane oxychlorination

Data for lanthanum content dependence of ethane conversion at 773 K are shown in figure 1, indicating that the conversion of ethane first tends to decrease, then increases with an increase in concentration of lanthanum. Over a catalyst containing 5 wt.% lanthanum (CuK5La), the conversion of ethane reaches a maximum. figure 2 shows the influence of lanthanum on the selectivity and yield of ethylene. It is worth to note that the selectivity and yield of ethylene over the CuK5La catalyst are lower than that over the others, but the selectivity for ethylene chloride is optimal (figure 3). The sum of the ethylene yield and ethylene chloride yield over this catalyst is almost unchanged with the concentration of lanthanum, implying that there is a competition between formations of the ethylene and ethylene chloride. The CuK5La catalyst shows the highest ethane conversion and ethylene chloride selectivity. We have investigated the initial activity and stability of the CuK5La catalyst, founding that no deactivation is detected within 100 h of time on stream over it. The conversion of ethane changes in a fluctuating mode between 88 and 92% and the sum of ethylene selectivity and ethylene chloride selectivity is higher than 70% (figures 4 and 5). The yield of ethyl chloride and 1,2-dichloroethane and carbon oxides increase gradually.

The catalytic process for the oxidative chlorination of ethane may be represented as follows [10]:

The reaction scheme suggests that the rate of oxidation increases and the rate of the dehydrochlorination of these compounds decreases. The used CuK5La catalyst can simply be regenerated in HCl and air atmosphere at 773 K and its catalytic properties can be recovered.

Turnover rate (TR) of ethane in it oxychlorination was calculated based on the data for ethane conversion, total flowrate of the reactant, ICP determination and XPS measurement. In this calculation, we referred to reference [11] the authors of which indicated that only highly dispersed anhydrous $CuCl_2$ is active for this

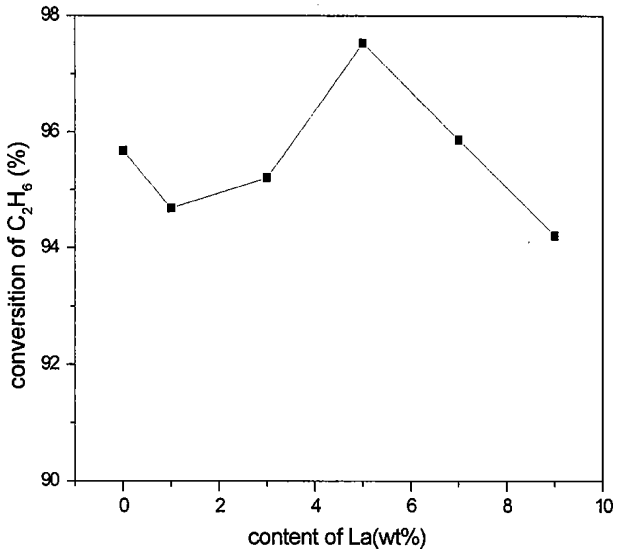

Figure 1. Influence of content of La on the conversion of ethane.

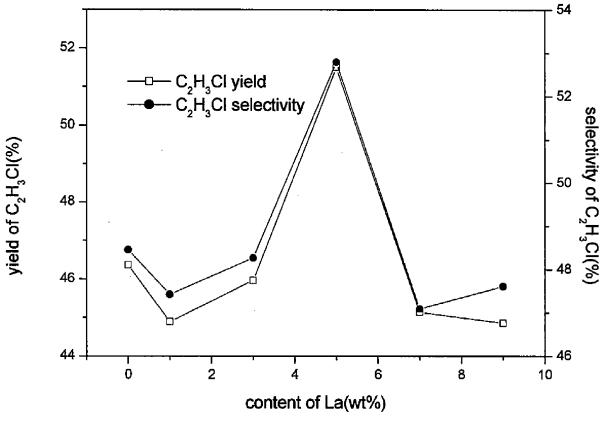

Figure 3. Influence of content of La on the yield and selectivity of C_2H_3Cl.

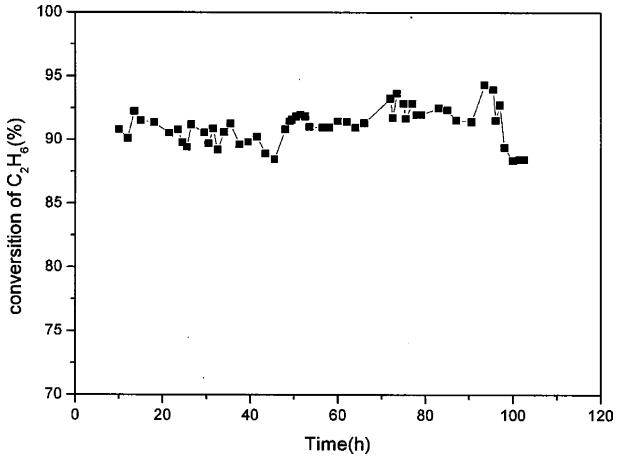

Figure 4. Change of C_2H_6 conversion with the reaction time on the CuK5La catalyst.

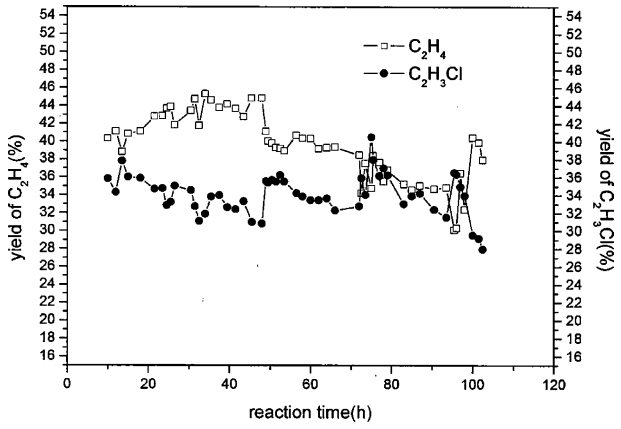

Figure 5. Change of C_2H_4 and C_2H_3Cl yield with the reaction time on the CuK5La catalyst.

reaction. The TRs of ethane over the fresh CuK5La catalyst and the catalyst used for 100 h are listed in table 1. From table 1, it can be seen that the TR of ethane almost keeps constant after 100 h of reaction.

3.2. The XRD patterns of catalysts

Figure 6 demonstrates the XRD patterns of the CuK5La catalyst used for different time. All the patterns clearly show that no diffraction peaks of copper chloride and lanthanum chloride appear, implying that these two compounds are highly dispersed. As it is stated that a threshold of $CuCl_2$ to form a monolayer on γ-Al_2O_3 is 18.98 wt.% [12,13] which is higher than the $CuCl_2$ content in these catalysts. $CuCl_2$ species in these catalysts are in the form of nanoclusters having a particle size of about 2–3 nm and are cannot be detected by X-ray diffraction [14]. However, diffraction peaks of KCl of the these catalysts are very apparent. With reaction time the peaks of KCl in the catalysts become weaker and become very small after 100 h of reaction, implying that its crystal is destroyed. This fact is probably because of the formation of KCl–$CuCl_2$ [15] which is also highly dispersed during the reaction.

3.3. Identification of the oxidation states of copper

As shown in figure 7(a), XPS spectrum of the fresh CuK5La catalyst shows a binding energy range of 925 eV through 960 eV. A peak at around 934.9 eV with a strong satellite peak originates from $Cu2p_{3/2}$ in $CuCl_2$, which is the active component for the ethane oxychlorination. The XPS spectrum of the catalyst used for 100 h and its fitted $Cu2p_{3/2}$ peaks are given in Figure7(b) and (c). It can be seen that there are two kinds of copper species on the surface of the used catalyst, the binding energies of which are 933.25 eV for Cu^+ and 935.46 eV for Cu^{2+} [16], respectively. In any case, formation of CuO and Cu_2O is impossible because an excess amount of HCl exists in the reaction, as schemed below:

$$2CuCl_2(s) \rightarrow Cu_2Cl_2(S) + Cl_2(g)$$

$$Cu_2Cl_2(s) + 1/2O_2(g) + 2HCl(g) \rightarrow 2CuCl_2(s) + H_2O(g)$$

Based on the fitted peaks of $Cu2p_{3/2}$, the presence of $CuCl_2$ and Cu_2C_{12} on the catalyst used for 100 h is verified.

Table 1
Ethane oxychlorination turnover rate on the CuK5La catalyst

	Reaction temperature (K)	TR ($\times 10^{-3}$ s^{-1})
Initial	773	6.31
100 h	773	6.96

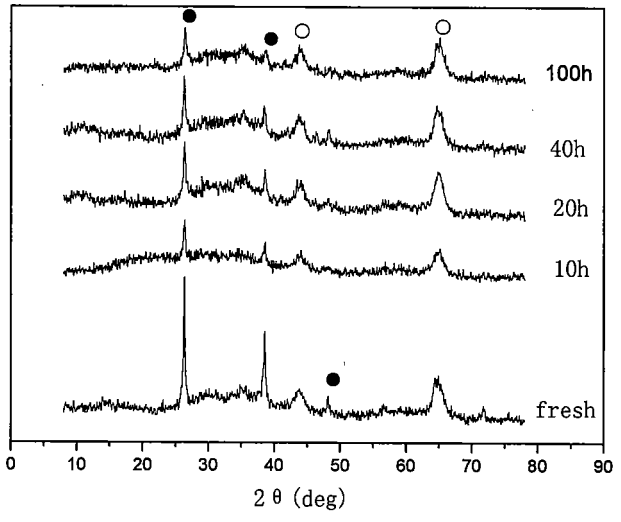

Figure 6. XRD patterns of CuK5La catalyst after reaction for different time ●, KCl; ○, γ-Al_2O_3.

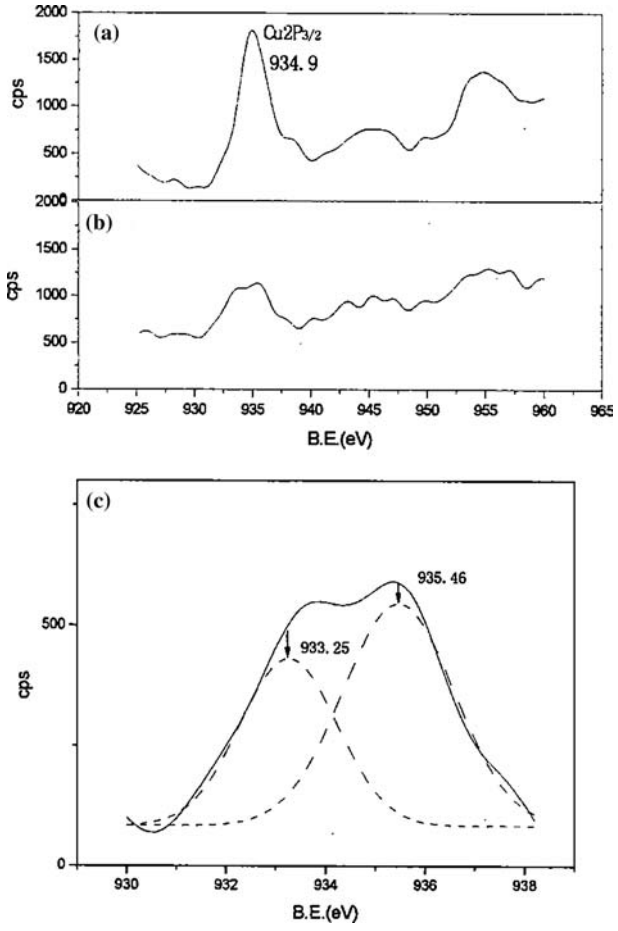

Figure 7. Cu(2p) X-ray photoelectron spectra of CuK5La (a) fresh catalyst (b) catalyst used for 100 h (c) enlarged (b) fitted Cu($2p_{3/2}$) photoelectron peaks of catalyst used for 100 h.

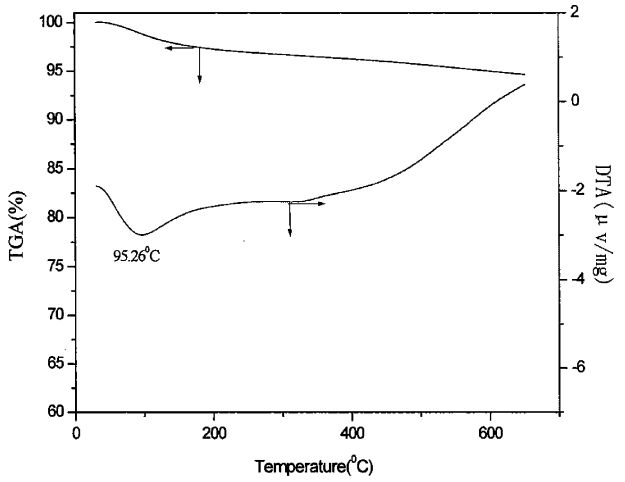

Figure 8. TGA/DTA curves of the fresh CuK5La catalyst.

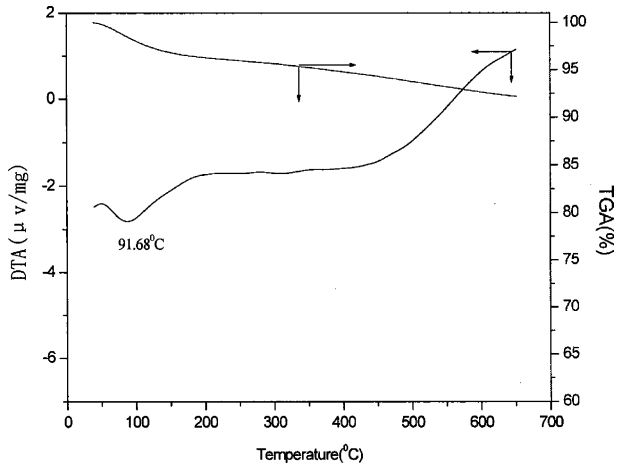

Figure 9. TGA/DTA curves of the CuK5La catalyst used for 20 h.

3.4. Carbon deposition of the CuK5La catalyst

The TGA profiles of the fresh and used CuK5La for 20, 40 and 100 h were measured, respectively as shown in figures 8–11. A small weight loss peak of about 2–3% at about 363 K appears in each catalyst regardless of being fresh or used for different time. This peak is due to water desorption. Over the CuK5La catalyst used for 20 h no peaks contributed to carbon deposition is seen, however, a large weight loss of about 5.92% at above 606 K is observed over the catalyst used for 40 h. Based upon the TGA/DTA profiles of the CuK5La catalyst the authors assume that the carbon deposition and ethane oxychlorination occur on different sites. The sites for carbon deposition are not intrinsic but form gradually. No carbon deposition is found after reaction for 20 h but the amount of deposited carbon further increases with the reaction time and after 100 h it reaches 12.5%. The peak corresponding to the combustion of the carbon in the used catalysts moves from 606 to 687 K with the reaction time from 40 to 100 h. The present authors assume that there exist two types of carbon species, one of which is active and another is relatively inert. The former, which dose not influence the catalytic properties, can be burned away during the reaction, but the latter, which affects the catalytic properties, can't be burned away at the reaction temperature. The carbon combustion temperature of the CuK5La catalyst used for 100 h is higher than that used for 40 h, indicating that the active carbon species is dominant in the latter case and the increase in the relatively inert species with reaction results in an increase in the carbon combustion temperature.

3.5. Specific surface area and pore size of the CuK5La catalyst

Data of specific surface area and average pore diameter of the CuK5La catalyst are given in table 2. It can be seen from table 2 that the specific surface area of the CuK5La catalyst decreases with the reaction time, but the average pore diameter increases within the

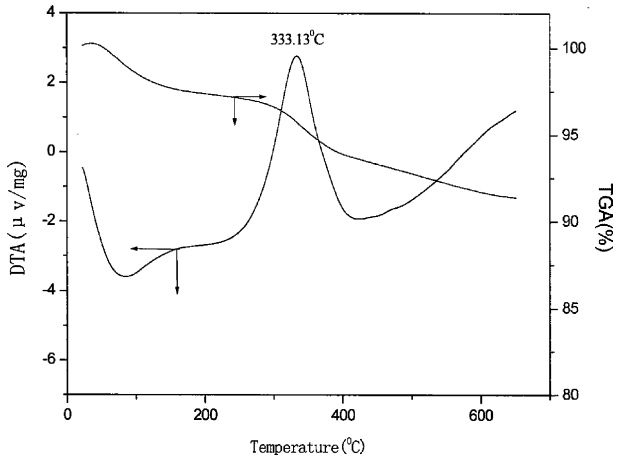

Figure 10. TGA/DTA curves of CuK5La catalyst used for 40 h.

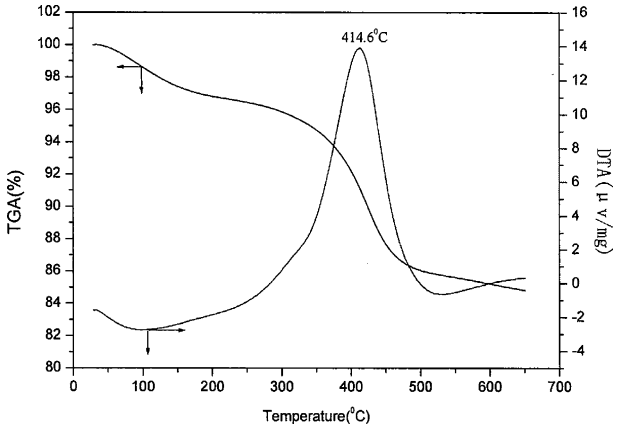

Figure 11. TGA/DTA curves of CuK5La catalyst used for 100 h.

first 20 h of reaction and decreases after 40 h. These results suggest that removal of active components from the pores of the catalyst occurred during the reaction, which led to an increase in the average pore diameter. But after 40 h of reaction carbon deposition takes place over the CuK5La catalyst so that pores of the catalyst may be blocked by the deposited carbon and become narrower. The results of the specific surface area and TGA/DTA determination of the CuK5La catalyst are coincident.

Data of the pore structure of the CuK5La catalyst after reaction for different periods of time are shown in figure 12. It can be concluded that the pore diameter of the catalyst is mainly distributed in a range of <10 nm and a maximum pore diameter of $\sim$6 nm is found after 10–40 h of reaction; but after 100 h of reaction it moves to <5 nm. Within a period of 40 h the pore diameter distribution of the CuK5La catalyst dose not change.

3.6. TEM measurements of catalysts

As shown in figure 13, the TEM profiles reveal the dispersion of the active species $CuCl_2$ on the catalyst surface, which are dispersed more uniformly (figure 13b) on the CuK5La catalyst than that on the La-free CuK catalyst (figure 13a). The reason for this fact may be

Table 2
Specific surface area and average pore diameter of the CuK5La catalyst

Reaction time	Fresh	10 h	20 h	40 h	100 h
BET (m^2/g)	71.46	68.46	66.03	66.40	61.87
Average pore diameter (nm)	6.11	6.34	6.57	6.00	5.70

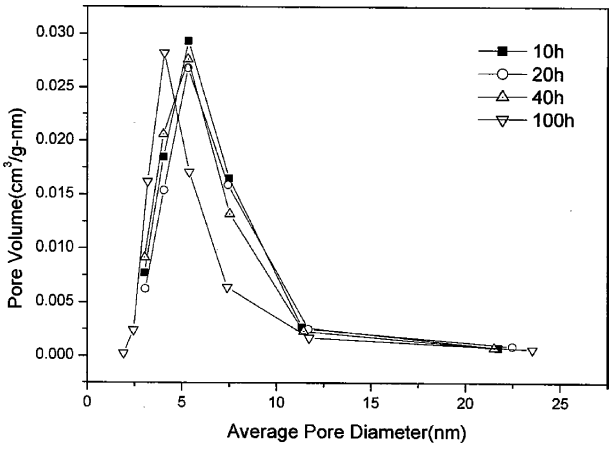

Figure 12. Pore diameter distribution of CuK5La after reaction of different periods of time.

that $CuCl_2$ particles are separated by lanthanum chloride. Thus, it can be concluded the addition of $LaCl_3$ can effectively prevent active species $CuCl_2$ from agglomeration and sintering, and make the catalyst more stable. figure 14 shows the TEM profile of the CuK5La catalyst after reaction of 100 h, from which it can be clearly seen that the used catalyst is sintered and its morphology is greatly changed.

3.7. ICP measurements of the CuK5La catalyst

The compositions of the fresh CuK5La catalyst and used catalysts are given in table 3. The data of ICP show that the contents of potassium and lanthanurn are slightly changed with increasing reaction time, but the concentration of Cu is decreased apparently after reaction, and only 3.8% of Cu was retained after 100 h of reaction. Correlating the change in the Cu content to the change in C_2H_3Cl and C_2H_4 yields with the reaction time on stream it can be found that a decrease in Cu content strongly effects on the C_2H_3Cl yield. Copper

Figure 14. TEM image of CuK5La catalyst used for 100 h.

chloride-based catalyst has some disadvantages, notably associated with its volatility at the reaction temperature. The present authors assume that a suitable ratio of Cu,

Table 3
Data of ICP for CuK5la catalyst after reaction for different time

Reaction time	Cu (wt.%)	K (wt.%)	La (wt.%)
Fresh	5.0	6.1	4.2
10 h	5.0	6.2	4.3
20 h	4.6	6.0	4.1
40 h	4.2	5.9	4.0
100 h	3.8	6.1	4.0

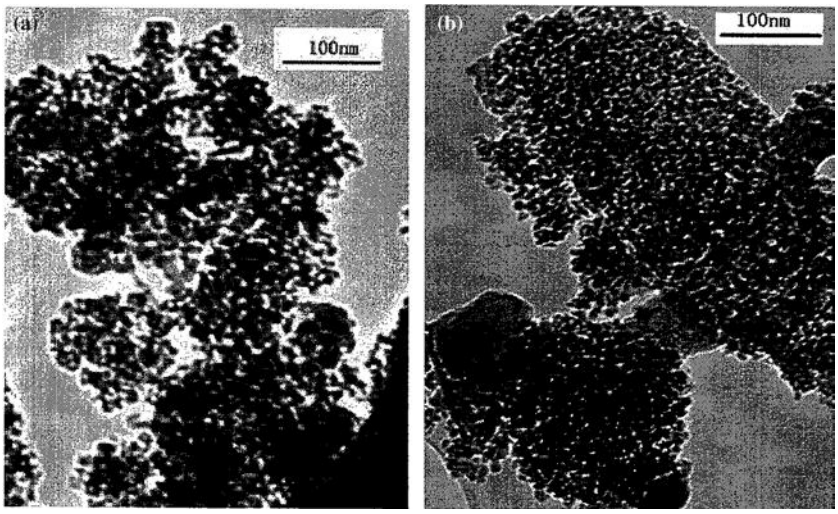

Figure 13. TEM image of fresh La-free CuK catalyst (a) and CuK5La catalyst (b).

K and La could make the volatility of copper chloride reduced.

Conclusions

1. Lanthanum of 5 wt.% doped 5 wt.%Cu–6 wt.%K/γ-Al_2O_3 catalyst shows the highest conversion of ethane and selectivity of ethylene chloride at 773 K.
2. TR of ethane almost keeps constant after 100 h of reaction.
3. Two reasons for the catalyst deactivation are suggested:
   (a) Carbon deposition on the catalyst surface.
   (b) Loss of active species of Cu^{2+}.
4. Carbon deposition begins after 40 h of reaction.
5. $LaCl_3$ as a promoter makes copper chloride highly dispersed and prevents effectively catalyst from sintering and agglomeration.

Acknowledgment

The authors greatly acknowledge the Science and Technology Department of Jilin Province for financial support (20020666).

References

[1] J.A. Allen and A.J. Clark, Rev. Pure Appl. Chem. 21 (1971) 145.
[2] C.N. Kenney, Catal. Rev. Sci. Eng. 11(2) (1975) 197.
[3] J. Villadsen and H. Livberg, Catal. Rev. Scv. Eng. 17(2) (1978) 203.
[4] J.S. Naworsky and E.S. Velez, *Applied Industrial Catalysis*, vol. 1 (Academic Press, San Diego, 1983), p. 239.
[5] Yu. A. Treger, V.N. Rozanov, M.R. Hid and L.M. Kartaschov, Vsp. Khim. 57(4) (1988) 577.
[6] H. Rigel, H.D. Schindler and M.C. Sze, Chem. Eng. Progr. 69(10) (1973) 89.
[7] J.A. Little and C.N. Kenney, J. Catal. 93 (1985) 23.
[8] Lǔ Xueju, Fei Qiang and Cheng Tiexin, et al., Chem. J. Chinese. Univ. 24 (2003) 522.
[9] M. Fernández-García, E. Gómez Rebollo and A. Guerrero Ruiz, et al., J. Catal. 172 (1997) 146.
[10] M.R. Flid, I.I. Kurlyandskaya and Yu.A. Treger, et al., *The Proceeding of 3rd World Congress on Oxidation Catalysis* (Elsevier Science B.V., San Diego, 1997) 305–313.
[11] G. Leofanti, M. Padovan and M. Garilli, et al., J. Catal. 189 (2000) 105.
[12] E. Finocchio, N. Rossi and G. Busca, et al., J. Catal. 179 (1998) 606.
[13] D. Carmello, E. Finocchio and A. Marsella, et al., J. Catal. 191 (2000) 354.
[14] G. Leofanti, M. Padovan and M. Garilli, et al., J. Catal. 189 (2000) 91.
[15] *Handbook of Chem. Phys.* 1981–1982 ed. Published by Chemical Rubber Company.
[16] V.K. Kaushik, Spectrochim. Acta 44B (1989) 581.